JACS
JOURNAL OF THE AMERICAN CHEMICAL SOCIETY

Communication

pubs.acs.org/JACS

Characterization of Indium Phosphide Quantum Dot Growth Intermediates Using MALDI-TOF Mass Spectrometry

Lisi Xie,[†,⊥] Yi Shen,[†,⊥] Daniel Franke,[‡] Víctor Sebastián,[§] Moungi G. Bawendi,*[,‡] and Klavs F. Jensen*[,†]

Departments of [†]Chemical Engineering and [‡]Chemistry, Massachusetts Institute of Technology, Cambridge, Massachusetts 02139, United States

[§]CIBER de Bioingeniería, Biomateriales y Nanomedicina (CIBER-BBN), Instituto Universitario de Nanociencia de Aragón, Department of Chemical Engineering, University of Zaragoza, Mariano Esquillor edif. I+D, Zaragoza 50018, Spain

Supporting Information

ABSTRACT: Clusters have been identified as important growth intermediates during group III–V quantum dot (QD) formation. Here we report a one-solvent protocol that integrates synthesis, purification, and mass characterization of indium phosphide (InP) QD growth mixtures. The use of matrix-assisted laser desorption/ionization (MALDI) mass spectrometry (MS) successfully tracks the evolution of clusters and the formation of QDs throughout the synthesis. Similar clusters are observed during the formation of large particles, suggesting that these clusters serve as a reservoir for QD formation. Combining MALDI and NMR techniques further enables us to extract extinction coefficients and construct sizing curves for cluster-free InP QDs. The use of MALDI MS opens new opportunities for characterization and mechanistic studies of small-sized air-sensitive clusters or QDs.

Quantum dots (QDs) have attracted significant attention[1] for applications spanning from optoelectronics[2] and photovoltaics[3] to biological imaging.[4] Colloidal indium phosphide (InP) nanocrystals stand out as the most promising Cd-free QD lighting and display materials.[5,6] Common syntheses of InP QDs utilize indium carboxylates and tris(trimethylsilyl)phosphine as precursors.[7] A two-step growth model has been proposed in which sub-nanometer clusters serve as important growth intermediates for the formation of larger InP nanocrystals.[8,9] While precursor conversion events have been investigated,[10−13] the formation mechanism of QDs from clusters remains disputed, with ripening,[14,15] coalescence,[14,15] and secondary nucleation[9] hypothesized as primary mechanisms.

Historically, absorbance measurements have been employed to monitor the growth of InP QDs.[8,9,11−13,15−19] However, as QDs possess larger absorption cross sections,[20−22] it is challenging to uncover the existence of clusters when QDs are also present. Their small size, close to 1 nm,[8,9] also makes clusters difficult to observe by other available methods, such as high-resolution transmission electron microscopy, dynamic light scattering, and small-angle X-ray scattering. Yet, to gain insights into InP QD growth from clusters, it is crucial to characterize cluster intermediates during nanocrystal formation.

As a soft ionization technique, matrix-assisted laser desorption/ionization time-of-flight (MALDI-TOF) mass spectrometry (MS) has been applied to studies of Au nanoclusters,[23,24] metal oxide nanoparticles,[25,26] and ZnS,[27] CdTe,[28] and CdSe[29,30] nanomaterials. It has also been used to characterize nonclassical growth mechanisms of inorganic nanoparticles.[31,32] MALDI MS requires samples to be co-crystallized with a matrix in a solid form. Since QD batch syntheses commonly utilize ligands or solvents with high boiling points, these nonvolatile impurities need to be completely removed in order to meet the MALDI vacuum requirements. In a typical QD purification process, polar solvents are added into the nonpolar growth solution to precipitate out the nanoparticles, during which the chemical identity of the surface QD atoms and/or surface ligands may be altered, or smaller clusters may be removed.[33−35] Moreover, InP cluster/QD surfaces are very sensitive to oxidation, especially when exposed to air.[36] These surface changes may affect the mass data and pose challenges in directly applying MALDI MS for characterizing InP growth intermediates.

Here we present an air-free, one-solvent method that allows us to synthesize InP QDs in a microfluidic reactor, to purify the resulting samples without precipitation, and to simultaneously track the formation of larger QDs and the consumption of smaller clusters via MALDI MS. Our results show that small InP clusters are formed right at the beginning of the synthesis and remain present throughout the entire process, thus acting as a reservoir for QD growth. Moreover, validated by MALDI MS, we construct a calibration curve relating particle mass and extinction coefficients of cluster-free QDs.

In our integrated approach, toluene is used as the solvent for synthesis, purification, and matrix preparation (Figure 1). Syntheses of InP growth intermediates are performed in high-temperature and high-pressure microchemical systems under inert conditions (Figure S1).[15,19] Purification of the intermediates is achieved by gel permeation chromatography (GPC)

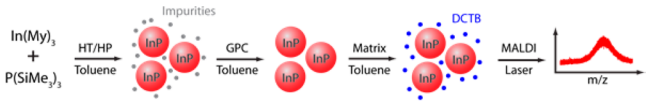

Figure 1. Integrated air-free approach to characterize InP QD growth mixtures using MALDI-TOF MS.

Received: June 22, 2016
Published: October 3, 2016

DOI: 10.1021/jacs.6b06468
J. Am. Chem. Soc. 2016, 138, 13469−13472

in a glovebox. GPC has been demonstrated to effectively remove unreacted precursors, ligands, and side products from QD growth solutions without perturbing the ligand-binding environment.[37,38] Moreover, both clusters and QDs elute out from the GPC column at the same time; therefore, they are preserved together in the purified solution. The absorption spectra of both clusters and QDs remain unchanged after GPC purification (Figure S2). ^{1}H and ^{31}P NMR spectra[39] before and after GPC purification show the effective removal of impurities and weakly associated ligands in the growth solution (Figure S3). The one-solvent, air-free synthesis and purification procedures allow us to obtain oxygen-free QDs for further mass characterization (Figure S4). *trans*-2-[3-(4-*tert*-Butylphenyl)-2-methyl-2-propenylidene]malononitrile (DCTB), a common MALDI matrix for metal clusters and nanoparticles,[24] is added to the purified InP–toluene solution. The InP–DCTB–toluene mixture is then spotted and dried on a MALDI plate in a glovebox. Both clusters and QDs are characterized at low laser powers in MALDI MS (Figure S5). Mass distributions obtained from MALDI correspond to UV–vis absorbance data, capturing the size change and size distribution of QDs with high resolution (Figure S6).

InP growth intermediates are first synthesized at different growth times and temperatures in a one-stage tube reactor system (Figure 2). Compared to the absorbance measurement,

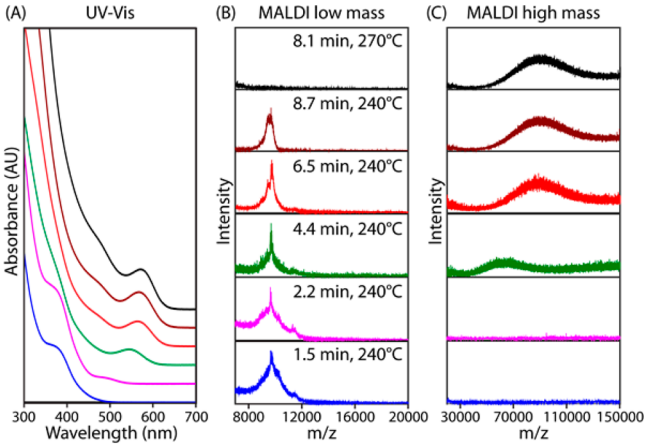

Figure 2. (A) UV–vis absorbance spectra and the corresponding (B) low-mass and (C) high-mass MALDI spectra of GPC-purified InP growth mixtures synthesized in a tube reactor. The growth time and temperature are provided in the middle panel for each condition.

MALDI spectra of the same InP growth mixtures not only provide information on the mass evolution of the larger particles but also reveal the existence of small cluster mixtures with masses around 10 kDa during the growth process. For the QD growth at 240 °C, similar clusters remain in the growth solution, while the QD mass increases from 60 kDa to close to 90 kDa (Figure 2 and Table S1). Surprisingly, clusters still exist even after 13 min of reaction time at 240 °C (Figure S7). Complete consumption of the clusters is achieved only for growth times longer than 8 min at 270 °C (Figure 2, top black curves, and Figure S7).

Similar clusters are also observed in two-step syntheses, where clusters are first formed at low temperatures and then used as precursors to form QDs at high temperatures. In a two-stage chip reactor system,[19] these small clusters show up after the precursor reaction in the first reactor at 130 °C (Figure S7) and then grow in a second reactor at temperatures between 180 and 300 °C (Figure 3). Although higher temperature results in

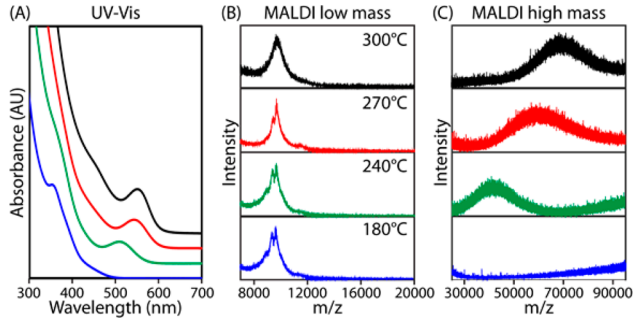

Figure 3. (A) UV–vis absorbance spectra and the corresponding (B) low-mass and (C) high-mass MALDI spectra of GPC-purified InP growth mixtures synthesized in a two-stage chip reactor system. The temperature of the first stage is 130 °C, and that of the second stage is shown in the middle panel for each condition.

the formation of larger QDs, these clusters are not yet fully consumed. These results are further confirmed in a conventional batch synthesis, in which similar cluster mixtures are formed at low temperatures (150 °C) and remain present throughout the growth at 230 °C (Figure S8).

Sub-nanometer InP clusters with an absorbance peak below 400 nm have been previously identified as important growth intermediates during the formation of InP QDs.[8,9] However, the UV absorption features of large nanocrystals in the growth mixtures can overshadow those of the clusters and thus hide their presence (Figures 2, 3, and S9). With MALDI MS, the clusters can be differentiated in the growth mixtures. Our observation of similar clusters in MALDI MS under different synthetic methods confirms their presence and stability during the growth of InP QDs. Moreover, the strong dependence of QD formation on the cluster's existence suggests their role as a continuous supply for the growth of larger InP nanocrystals. In fact, InP QDs can be prepared with the purified clusters as the only source for growth (Figure S10), implying that QD growth can occur solely via clusters as intermediates rather than mixtures of clusters and the initial molecular precursors.

The stability of InP clusters poses challenges to prepare cluster-free QDs with varying sizes by simply adjusting growth temperature and time. As clusters absorb in the UV region, their existence can also affect the results of optical studies of InP QDs. Our study shows that high temperature and long reaction times are essential to prepare cluster-free InP QDs. In order to tune the size of cluster-free QDs, various concentrations of TOP and TOPO (Table S2) are added to reaction mixtures, and this results in QD samples with first absorption peaks ranging from 520.5 to 579.5 nm (Figure 4). MALDI spectra of these solutions at low mass show no detectable clusters (Figure S11), while high-mass characterization maps out QD masses ranging from 46.5 to 99.0 kDa.

In order to validate the accuracy of MALDI mass against particle size, two cluster-free QD solutions with their first absorption peaks at 520 and 580 nm are chosen (protocol available in the Supporting Information (SI)). ^{1}H and ^{31}P NMR show that myristate is the only organic ligand species bound to the purified QDs. The inorganic core mass can then be obtained by subtracting the myristate mass from the particle mass (Table S3). The volume of the inorganic core is obtained by assuming that its density is the same as that of the bulk InP.

DOI: 10.1021/jacs.6b06468
J. Am. Chem. Soc. 2016, 138, 13469–13472

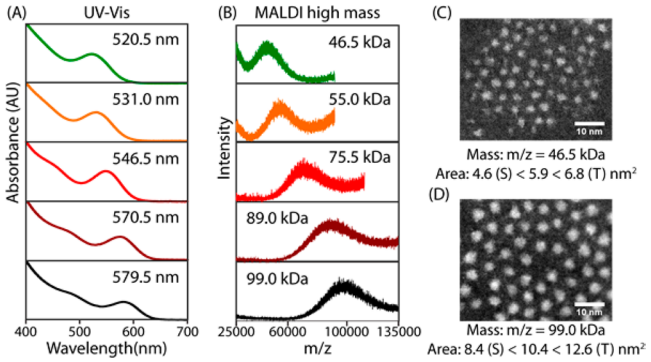

Figure 4. (A) UV−vis absorbance and (B) high-mass MALDI MS spectra of GPC-purified cluster-free InP QDs synthesized in a tube reactor at 270 °C. STEM-HAADF image of InP QDs with the first absorption peak at (C) 520.5 and (D) 579.5 nm. For the projected area calculations per particle, middle number is from STEM, left number is from MALDI assuming spherical (S) shape, and right number is from MALDI assuming tetrahedral (T) shape.

Since InP QDs have been observed in both nearly spherical (S) and tetrahedral (T) shapes,[12,38,40] the projected area corresponding to either shape is calculated from the volume of the inorganic core and compared with that obtained from scanning transmission electron microscopy−high-angle annular dark-field imaging (STEM-HAADF) analysis (Figures 4 and S12, and Table S3). While MALDI MS is known to cause the possible fragmentation of CdSe nanoparticles,[41,42] good agreement is achieved between MALDI and STEM characterization, confirming the accuracy of MALDI in determining InP QD mass.

The synthesis of cluster-free InP QD samples further allows us to extract molar extinction coefficients and size-dependent absorption calibration curves of QDs, which are essential for studies concerning nanocrystal concentrations and sizes.[20−22] With MALDI MS, the extinction coefficient of a QD sample can be quantified by measuring its absorption and then determining its concentration by dividing the QD dry mass by the MALDI particle mass. No assumption is made on the particle density or shape. However, to provide a reference value of the particle size, a certain shape is assumed to calculate the projected area of the particles.

In the manner outlined above (detailed calculations including error estimation are given in the SI and Table S3), the extinction coefficients of a series of cluster-free InP QDs at 310 nm are determined (Table 1). The mass information combined with proton quantification through NMR is also used to obtain the number of ligands and InP units per particle (Table 1). As previous studies have indicated, the extinction coefficients of QDs scale linearly with their effective nanoparticle volume,[11] and namely the number of molecule units per particle. This scaling factor is found to be around 5100 M^{-1} cm^{-1} for InP QDs evaluated in our work (Table 1 and Figure S13; calculation available in SI). The estimated absorption cross section of QDs at 310 nm also agrees well with that of the bulk material (see SI). We have also evaluated the extinction coefficients at 350 nm to compare with available literature results, and good agreement for InP QDs with similar sizes is observed (Figure S14).[43]

Table 1. Cluster-Free QDs with Their First Absorption Peaks, Their Estimated Number of Ligands and InP Units, and Their Extinction Coefficients Per Particle (ε) and per InP Unit (ε') at 310 nm

first abs peak (nm)	no. of ligands	no. of InP units	ε (M^{-1} cm^{-1})	ε' (M^{-1} cm^{-1})
520.5	111	117	6.0×10^5	5.1×10^3
531.0	130	141	7.1×10^5	5.0×10^3
546.5	157	198	10.2×10^5	5.2×10^3
570.5	185	274	14.3×10^5	5.2×10^3
579.5	201	313	16.1×10^5	5.1×10^3

In conclusion, we have developed an integrated air-free protocol to characterize InP QD growth intermediates using MALDI-TOF MS. This method allows for differentiating the signals of clusters and QDs, yielding important insights into InP QD growth. Interestingly, similar clusters are persistent during the QD growth, suggesting their role as a supply for the formation of larger InP particles. Validated by MALDI MS, cluster-free InP QDs with different sizes are synthesized to construct a correlation between the absorption features and the mass/concentration of InP QDs. Our protocol using MALDI MS thus provides new opportunities in characterizing and understanding the growth mechanism underlying small-sized air-sensitive clusters or QDs.

■ ASSOCIATED CONTENT

Supporting Information

The Supporting Information is available free of charge on the ACS Publications website at DOI: 10.1021/jacs.6b06468.

Experimental details, quantification methods, STEM analysis, ^{1}H and ^{31}P NMR spectra and UV−vis spectra of InP growth intermediates before and after GPC purification, MALDI spectra of clusters and QDs at different laser powers, additional UV−vis and MALDI spectra of InP QDs grown in tube and batch reactors, and low-mass MALDI characterization of cluster-free InP QDs, including Figures S1−S14 and Tables S1−S3 (PDF)

■ AUTHOR INFORMATION

Corresponding Authors

*mgb@mit.edu
*kfjensen@mit.edu

Author Contributions

⊥L.X. and Y.S. contributed equally.

Notes

The authors declare no competing financial interest.

■ ACKNOWLEDGMENTS

This work was supported by the National Science Foundation under grant no. ECCS-1449291. D.F. was supported by a Boehringer Ingelheim Fonds fellowship. V.S. acknowledges financial support from EU CIG−Marie Curie under REA grant agreement no. 321642. We thank Alla Leshinsky and Richard F. Cook in the Biopolymers and Proteomics Core in Koch Institute in MIT for the MALDI-TOF MS characterization. We thank Prof. Strano for the use of the UV−vis spectrometer in his laboratory. We thank Li Li in DCIF and Mark Simon in the Pentelute Lab for helpful discussions related to MALDI MS. We thank Maggie He and Bing Yan for the XPS measurements.

DOI: 10.1021/jacs.6b06468
J. Am. Chem. Soc. 2016, 138, 13469−13472

REFERENCES

(1) Kovalenko, M. V.; Manna, L.; Cabot, A.; Hens, Z.; Talapin, D. V.; Kagan, C. R.; Klimov, V. I.; Rogach, A. L.; Reiss, P.; Milliron, D. J.; Guyot-Sionnnest, P.; Konstantatos, G.; Parak, W. J.; Hyeon, T.; Korgel, B. A.; Murray, C. B.; Heiss, W. *ACS Nano* **2015**, *9*, 1012.
(2) Talapin, D. V.; Lee, J.-S.; Kovalenko, M. V.; Shevchenko, E. V. *Chem. Rev.* **2010**, *110*, 389.
(3) Carey, G. H.; Abdelhady, A. L.; Ning, Z.; Thon, S. M.; Bakr, O. M.; Sargent, E. H. *Chem. Rev.* **2015**, *115*, 12732.
(4) Medintz, I. L.; Uyeda, H. T.; Goldman, E. R.; Mattoussi, H. *Nat. Mater.* **2005**, *4*, 435.
(5) Wood, V.; Bulović, V. *Nano Rev.* **2010**, *1*, 5202.
(6) Chen, O.; Wei, H.; Maurice, A.; Bawendi, M.; Reiss, P. *MRS Bull.* **2013**, *38*, 696.
(7) Tamang, S.; Lincheneau, C.; Hermans, Y.; Jeong, S.; Reiss, P. *Chem. Mater.* **2016**, *28*, 2491.
(8) Gary, D. C.; Flowers, S. E.; Kaminsky, W.; Petrone, A.; Li, X.; Cossairt, B. M. *J. Am. Chem. Soc.* **2016**, *138*, 1510.
(9) Gary, D. C.; Terban, M. W.; Billinge, S. J. L.; Cossairt, B. M. *Chem. Mater.* **2015**, *27*, 1432.
(10) Xie, L.; Zhao, Q.; Jensen, K. F.; Kulik, H. J. *J. Phys. Chem. C* **2016**, *120*, 2472.
(11) Harris, D. K.; Bawendi, M. G. *J. Am. Chem. Soc.* **2012**, *134*, 20211.
(12) Gary, D. C.; Glassy, B. A.; Cossairt, B. M. *Chem. Mater.* **2014**, *26*, 1734.
(13) Franke, D.; Harris, D. K.; Xie, L.; Jensen, K. F.; Bawendi, M. G. *Angew. Chem.* **2015**, *127*, 14507.
(14) Allen, P. M.; Walker, B. J.; Bawendi, M. G. *Angew. Chem., Int. Ed.* **2010**, *49*, 760.
(15) Baek, J.; Allen, P. M.; Bawendi, M. G.; Jensen, K. F. *Angew. Chem., Int. Ed.* **2011**, *50*, 627.
(16) Battaglia, D.; Peng, X. *Nano Lett.* **2002**, *2*, 1027.
(17) Gary, D. C.; Cossairt, B. M. *Chem. Mater.* **2013**, *25*, 2463.
(18) Tessier, M. D.; Dupont, D.; De Nolf, K.; De Roo, J.; Hens, Z. *Chem. Mater.* **2015**, *27*, 4893.
(19) Xie, L.; Harris, D. K.; Bawendi, M. G.; Jensen, K. F. *Chem. Mater.* **2015**, *27*, 5058.
(20) Jasieniak, J.; Smith, L.; van Embden, J.; Mulvaney, P.; Califano, M. *J. Phys. Chem. C* **2009**, *113*, 19468.
(21) Leatherdale, C. A.; Woo, W. K.; Mikulec, F. V.; Bawendi, M. G. *J. Phys. Chem. B* **2002**, *106*, 7619.
(22) Yu, W. W.; Qu, L.; Guo, W.; Peng, X. *Chem. Mater.* **2003**, *15*, 2854.
(23) Levi-Kalisman, Y.; Jadzinsky, P. D.; Kalisman, N.; Tsunoyama, H.; Tsukuda, T.; Bushnell, D. A.; Kornberg, R. D. *J. Am. Chem. Soc.* **2011**, *133*, 2976.
(24) Dass, A.; Stevenson, A.; Dubay, G. R.; Tracy, J. B.; Murray, R. W. *J. Am. Chem. Soc.* **2008**, *130*, 5940.
(25) Guan, B.; Lu, W.; Fang, J.; Cole, R. B. *J. Am. Soc. Mass Spectrom.* **2007**, *18*, 517.
(26) Kim, B. H.; Shin, K.; Kwon, S. G.; Jang, Y.; Lee, H.-S.; Lee, H.; Jun, S. W.; Lee, J.; Han, S. Y.; Yim, Y.-H.; Kim, D.-H.; Hyeon, T. *J. Am. Chem. Soc.* **2013**, *135*, 2407.
(27) Khitrov, G. A.; Strouse, G. F. *J. Am. Chem. Soc.* **2003**, *125*, 10465.
(28) Li, J.; Yang, T.; Chan, W. H.; Choi, M. M. F.; Zhao, D. *J. Phys. Chem. C* **2013**, *117*, 19175.
(29) Yang, J.; Fainblat, R.; Kwon, S. G.; Muckel, F.; Yu, J. H.; Terlinden, H.; Kim, B. H.; Iavarone, D.; Choi, M. K.; Kim, I. Y.; Park, I.; Hong, H.-K.; Lee, J.; Son, J. S.; Lee, Z.; Kang, K.; Hwang, S.-J.; Bacher, G.; Hyeon, T. *J. Am. Chem. Soc.* **2015**, *137*, 12776.
(30) Muckel, F.; Yang, J.; Lorenz, S.; Baek, W.; Chang, H.; Hyeon, T.; Bacher, G.; Fainblat, R. *ACS Nano* **2016**, *10*, 7135.
(31) Wang, F.; Richards, V. N.; Shields, S. P.; Buhro, W. E. *Chem. Mater.* **2014**, *26*, 5.
(32) Lee, J.; Yang, J.; Kwon, S. G.; Hyeon, T. *Nature Reviews Materials* **2016**, *1*, 16034.
(33) Morris-Cohen, A. J.; Donakowski, M. D.; Knowles, K. E.; Weiss, E. A. *J. Phys. Chem. C* **2010**, *114*, 897.
(34) Shakeri, B.; Meulenberg, R. W. *Langmuir* **2015**, *31*, 13433.
(35) Anderson, N. C.; Hendricks, M. P.; Choi, J. J.; Owen, J. S. *J. Am. Chem. Soc.* **2013**, *135*, 18536.
(36) Cros-Gagneux, A.; Delpech, F.; Nayral, C.; Cornejo, A.; Coppel, Y.; Chaudret, B. *J. Am. Chem. Soc.* **2010**, *132*, 18147.
(37) Shen, Y.; Gee, M. Y.; Tan, R.; Pellechia, P. J.; Greytak, A. B. *Chem. Mater.* **2013**, *25*, 2838.
(38) Shen, Y.; Roberge, A.; Tan, R.; Gee, M. Y.; Gary, D. C.; Huang, Y.; Blom, D. A.; Benicewicz, B. C.; Cossairt, B. M.; Greytak, A. B. *Chem. Sci.* **2016**, *7*, 5671.
(39) Hens, Z.; Martins, J. C. *Chem. Mater.* **2013**, *25*, 1211.
(40) Kim, K.; Yoo, D.; Choi, H.; Tamang, S.; Ko, J.-H.; Kim, S.; Kim, Y.-H.; Jeong, S. *Angew. Chem., Int. Ed.* **2016**, *55*, 3714.
(41) Wang, Y. L.; Liu, Y.-H.; Zhang, Y.; Wang, F.; Kowalski, P. J.; Rohrs, H. W.; Loomis, R. A.; Gross, M. L.; Buhro, W. E. *Angew. Chem., Int. Ed.* **2012**, *51*, 6154.
(42) Beecher, A. N.; Yang, X.; Palmer, J. H.; LaGrassa, A. L.; Juhas, P.; Billinge, S. J. L.; Owen, J. S. *J. Am. Chem. Soc.* **2014**, *136*, 10645.
(43) Talapin, D. V.; Gaponik, N.; Borchert, H.; Rogach, A. L.; Haase, M.; Weller, H. *J. Phys. Chem. B* **2002**, *106*, 12659.

DOI: 10.1021/jacs.6b06468
J. Am. Chem. Soc. 2016, 138, 13469−13472